



Published in final edited form as:

*Hepatology*. 2020 June ; 71(6): 1923–1939. doi:10.1002/hep.30959.

## Crigler-Najjar Syndrome Type 1: Pathophysiology, Natural History, and Therapeutic Frontier

Kevin A. Strauss<sup>1,2,3</sup>, Charles E. Ahlfors<sup>4</sup>, Kyle Soltys<sup>5</sup>, George V. Mazareigos<sup>5</sup>, Millie Young<sup>1</sup>, Lauren E. Bowser<sup>1</sup>, Michael D. Fox<sup>1,6,7</sup>, James E. Squires<sup>8</sup>, Patrick McKiernan<sup>9</sup>, Karlla W. Brigatti<sup>1</sup>, Erik G. Puffenberger<sup>1</sup>, Vincent J. Carson<sup>1</sup>, Hendrik J. Vreman<sup>10</sup>

<sup>1</sup>Clinic for Special Children, Strasburg, PA

<sup>2</sup>Penn-Lancaster General Hospital, Lancaster, PA

<sup>3</sup>Departments of Pediatrics and Molecular, Cell & Cancer Biology, University of Massachusetts School of Medicine, Worcester, MA

<sup>4</sup>Department of Pediatrics, Stanford University School of Medicine, Stanford, CA

<sup>5</sup>Department of Surgery, Division of Pediatric Transplantation, Hillman Center for Pediatric Transplantation, UPMC Children's Hospital of Pittsburgh, Pittsburgh, PA

<sup>6</sup>Department of Pediatrics, Sidney Kimmel Medical College at Thomas Jefferson University, Philadelphia, PA

<sup>7</sup>Diagnostic Referral Division, Nemours/Alfred I. duPont Hospital for Children, Wilmington, DE

<sup>8</sup>Division of Gastroenterology and Hepatology, Department of Pediatrics, UPMC Children's Hospital of Pittsburgh, Pittsburgh, PA

<sup>9</sup>Division of Pediatric Gastroenterology, Hepatology and Nutrition, UPMC Children's Hospital of Pittsburgh and Pittsburgh Liver Research Center, Pittsburgh, PA

<sup>10</sup>Division of Neonatal and Developmental Medicine, Department of Pediatrics, Stanford University School of Medicine, Stanford, CA.

### Abstract

**BACKGROUND AND AIMS:** We describe the pathophysiology, treatment, and outcome of Crigler-Najjar type 1 syndrome (CN1) in 28 *UGT1A1 c.222C>A* homozygotes followed for 520 aggregate patient-years.

**ADDRESS CORRESPONDENCE AND REPRINT REQUESTS TO:** Kevin A. Strauss, M.D., Clinic for Special Children, 535 Bunker Hill Road, Strasburg, PA 17579, kstrauss@clinicforspecialchildren.org, Tel.: +1-717-687-9407.

**Author Contributions:** K.A.S. conceptualized and supervised the project and contributed to formal analysis, methodology, investigation, visualization, and writing of the manuscript. Other authors who contributed substantially to methodology, investigation, and formal analysis include C.E.F., K.S., G.V.M., E.G.P., and H.J.V. M.Y., L.E.B., M.D.F., J.E.S., and P.M. curated data and contributed to formal analysis and visualization. K.W.B. served as project administrator and supervised data curation. The original draft was written by K.A.S., M.D.F., and E.G.P. Substantive manuscript review, editing, and revision was provided by C.E.F., V.J.C., and H.J.V. H.J.V. designed and constructed light-emitting diode-based phototherapy systems.

Potential conflict of interest: The Clinic for Special Children received grants from Audentes.

Supporting Information

Additional Supporting Information may be found at [onlinelibrary.wiley.com/doi/10.1002/hep.30959/supinfo](https://onlinelibrary.wiley.com/doi/10.1002/hep.30959/supinfo).

**APPROACH AND RESULTS:** Unbound (“free”) bilirubin ( $B_f$ ) was measured in patient sera to characterize the binding of unconjugated bilirubin ( $B_T$ ) to albumin (A) and validate their molar concentration ratio ( $B_T/A$ ) as an index of neurological risk. Two custom phototherapy systems were constructed from affordable materials to provide high irradiance in the outpatient setting; light dose was titrated to keep  $B_T/A$  at least 30% below intravascular  $B_T$  binding capacity (i.e.,  $B_T/A = 1.0$ ). Categorical clinical outcomes were ascertained by chart review, and a measure ( $L_f$ ) was used to quantify liver fibrosis. Unbound bilirubin had a nonlinear relationship to  $B_T$  ( $R^2 = 0.71$ ) and  $B_T/A$  ( $R^2 = 0.76$ ), and  $B_f$  as a percentage of  $B_T$  correlated inversely to the bilirubin–albumin equilibrium association binding constant ( $R^2 = 0.69$ ), which varied 10-fold among individuals. In newborns with CN1, unconjugated bilirubin increased  $4.3 \pm 1.1$  mg/dL per day. Four (14%) neonates developed kernicterus between days 14 and 45 postnatal days of life; peak  $B_T$  30 mg/dL and  $B_T/A$  1.0 mol:mol were equally predictive of perinatal brain injury (sensitivity 100%, specificity 93.3%, positive predictive value 88.0%), and starting phototherapy after age 13 days increased this risk 3.5-fold. Consistent phototherapy with  $33\text{--}103 \mu\text{W}/\text{cm}^2 \cdot \text{nm}$  for  $9.2 \pm 1.1$  hours/day kept  $B_T$  and  $B_T/A$  within safe limits throughout childhood, but  $B_T$  increased 0.46 mg/dL per year to reach dangerous concentrations by 18 years of age. Liver transplantation ( $n = 17$ ) normalized  $B_T$  and eliminated phototherapy dependence. Liver explants showed fibrosis ranging from mild to severe.

**CONCLUSION:** Seven decades after its discovery, CN1 remains a morbid and potentially fatal disorder. (HEPATOLOGY 2020;71:1923-1939).

In 1952, John Crigler and Victor Najjar described 7 infants from three families who developed intractable nonhemolytic jaundice within the first week of life<sup>(1)</sup>; 6 died of bilirubin encephalopathy by 15 months of age. Crigler-Najjar syndrome (OMIM 218800) was subsequently linked to deficiency of hepatic uridine 5'-diphosphate glucuronyltransferase (UGT1A1),<sup>(2)</sup> which mediates the glucuronidation of 4Z,15Z-bilirubin requisite for its biliary excretion (Fig. 1).<sup>(3)</sup> Residual UGT1A1 activity and its inducibility by phenobarbital allow distinction among type 1 (CN1; absence of UGT1A1), type 2 (CN2; 4%-10% UGT1A1), and type 3 (CN3; 20%-30% UGT1A1; Gilbert syndrome) clinical variants (OMIM PS237450).

Native bilirubin is a degradation product of heme, and in the absence of hepatic UGT1A1 activity, accumulates in humans at a relatively constant rate of  $3.8 \pm 0.6$  mg/kg per day.<sup>(4)</sup> Unconjugated bilirubin has low aqueous solubility at physiological pH ( $\sim 70$  nmol/L; 4  $\mu\text{g}/\text{dL}$ ),<sup>(5)</sup> and moves in chemical equilibria between a limited number of high-affinity binding sites on albumin and a much larger reservoir of low-affinity sites on erythrocytes, adipocytes, and endothelial cells (Fig. 1).<sup>(6)</sup> *In vivo*, more than 99% of intravascular unconjugated bilirubin ( $B_T$ ) is bound to albumin and interacts minimally with cerebral endothelia.<sup>(7)</sup> In contrast, unbound (“free”) bilirubin ( $B_f$ ) readily crosses the blood–brain barrier and binds to neural membranes.<sup>(8,9)</sup> As intravascular binding capacity saturates,  $B_f$  increases as a proportion of the total, driving pigment deposition in brain and other extravascular tissues.

The quantity of bilirubin bound to brain tissue correlates directly with indices of cellular dysfunction and injury.<sup>(9-11)</sup> In humans, diminished amplitude and velocity of auditory

brainstem responses (ABR) are the earliest signs of bilirubin encephalopathy and correlate more closely with  $B_f$  than  $B_T$ .<sup>(12,13)</sup> A critical threshold of cerebral pigment deposition causes kernicterus (German *kern* [“nucleus”] and *ikterus* [“jaundice”]), a devastating static encephalopathy marked by staining of cranial nerve, subthalamic, basal ganglia, and hippocampal neurons that manifests as sudden neurological regression followed by generalized dystonia, choreoathetosis, ataxia, oculomotor palsy, seizures, or death.<sup>(14)</sup> The advent of effective phototherapy systems between 1958 and 1968<sup>(15,16)</sup> afforded CN1 patients a mechanism of protection from this catastrophic outcome.<sup>(17)</sup>

Crigler-Najjar syndrome type 1 is exceedingly rare worldwide (~1 per 1,000,000 live births) but unusually common among the Old Order Amish and Mennonite (Plain) people, who descended from just a few hundred Swiss-German Anabaptists and now comprise about 800,000 individuals inhabiting isolated demes throughout North and South America. A pathogenic missense variant of *UGT1A1* (c.222C>A; p.Tyr74\*) was introduced separately into Amish and Mennonite populations approximately 300 years ago and likely arose in a common ancestor more than 1,000 years before the formation of the Anabaptist church. The *UGT1A1* c.222C>A variant has drifted to allele frequencies of 2.17% (incidence of 1 per 2,124 births) and 0.83% (incidence of 1 per 14,520 births) within extant Mennonite (Weaverland and Groffdal Conferences) and Old Lancaster Amish populations, respectively.

Here, we describe the clinical course, treatment, and outcome of 28 *UGT1A1* c.222C>A homozygotes with a severe (type 1) biochemical phenotype over 30 years of follow-up. This study extends the findings of a report published in 2006,<sup>(17)</sup> which included 17 *UGT1A1* c.222C>A homozygotes managed at our center in Pennsylvania (Clinic for Special Children; CSC). We provide a status update on these 17 patients and include new data about 11 additional *UGT1A1* c.222C>A homozygotes, 7 of whom were managed at other Midwestern U.S. sites. Our longitudinal observations over 3 decades yield insights into the pathophysiology of bilirubin encephalopathy, underscore principles of effective phototherapy, and provide a framework against which to judge emerging molecular therapies for CN1 and other inborn errors of liver metabolism.

## Materials and Methods

### PATIENTS

The study was approved by the Penn-Lancaster General Hospital Institutional Review Board, and patients or their parents consented in writing to participate. The CSC database contained 28 *UGT1A1* c.222C>A homozygotes (48% female) born between 1984 and 2015 (median age 19.2, range 3.2-34.7 years) and comprised of 520 aggregate patient-years of follow-up. Twenty-one (75%) individuals were followed clinically at CSC<sup>(17)</sup> and are joined in the present report by 7 additional patients managed at other sites in the Midwestern United States. All patients had a severe (type 1) clinical phenotype, defined here as unconjugated hyperbilirubinemia unresponsive to phenobarbital and necessitating 7 or more hours of high-intensity phototherapy daily to maintain serum bilirubin below a neurotoxic threshold. Based on converging lines of evidence, we define  $B_T \leq 30$  mg/dL (513  $\mu$ mol/L) and  $B_T/A \leq 1.0$  mol: mol as absolute thresholds for neurotoxicity *in vivo*. However, to safeguard patients against approaching these limits, we try to keep  $B_T$  and  $B_T/A$

approximately 30% lower, at 20 mg/dL (340  $\mu$ mol/L) and 0.7 mol:mol, respectively. During severe exacerbations of hyperbilirubinemia, patients were managed according to a standard inpatient protocol that included a provision for intravenous albumin infusions (Table 1).

## BILIRUBIN KINETICS, BIODISTRIBUTION, AND RISK ASSESSMENT

Using  $B_T$  values from newborns naïve to phototherapy, we calculated the postnatal rate of bilirubin formation (mg/kg per day) based on the following assumptions: (1) In the absence of UGT1A1 activity and photoisomerization, unconjugated bilirubin excretion is negligible; (2) the plasma compartment represents about 40 mL/kg body weight; and (3) in jaundiced patients, the total bilirubin load is about equally distributed between intravascular and extravascular binding sites.<sup>(13)</sup>

The plasma concentration of  $B_f$  is more closely linked to neuronal injury than  $B_T$ , but is a challenging parameter to measure and not widely available for clinical use.<sup>(13)</sup> We therefore used the serum  $B_T/A$  molar concentration ratio (mol:mol) as a surrogate for  $B_f$ , and thereby an index of neurological risk in which 1 g of human albumin (molecular weight [MW] 66,437 g/mol) binds approximately 9 mg of bilirubin (MW 584.7 g/mol) (<https://www.sigmaaldrich.com>) with a stoichiometry of about 1:1, and their mass units are converted to concentrations in  $\mu$ mol/L as follows (Fig. 1):

$$\frac{B_T \text{ in } \mu\text{mol} / \text{L}}{A \text{ in } \mu\text{mol} / \text{L}} = \frac{17.1 (B_T \text{ in mg} / \text{dL})}{151 (A \text{ in g} / \text{dL})} \quad (1)$$

The relationship between  $B_T$  and  $B_f$  is expressed by the following mass action equation:

$$B_f = \frac{(B_T - B_f)}{K(P - B_T + B_f)}, \quad (2)$$

where P represents the concentration of intravascular protein binding sites ( $\mu$ mol/L) and K is the bilirubin–protein equilibrium association binding constant (L/ $\mu$ mol). In practice, the overwhelming majority of binding sites are represented by albumin (A), and K is effectively the equilibrium association binding constant of the bilirubin–albumin complex. Within clinically relevant values of  $B_T$  and A,  $B_f$  is less than 0.01% of  $B_T$  and can be ignored, which simplifies the mass action equilibrium to

$$B_f = \frac{B_T}{K(A - B_T)}. \quad (3)$$

Various ligands (e.g., drugs, preservatives, contrast agents) alter the relationship between  $B_T$  and  $B_f$  by directly reducing the number of available binding sites or causing conformational changes of albumin that indirectly reduce the binding constant (Fig. 1).

To validate these relationships for clinical practice, we measured  $B_f$  from serum of 18 *UGT1A1* c.222C>A homozygotes and 7 healthy Amish control individuals on the Arrows UB-analyzer (Arrows Co. Ltd., Osaka, Japan) using the horseradish peroxidase (HRP)

method as previously described.<sup>(18)</sup> The assay was run at two different HRP concentrations to accurately determine equilibrium  $B_f$ , and Eq. 3 was used to calculate K for each sample. Results were compared with available data from two high-risk populations: 6 preterm neonates weighing less than 1.0 kg who received an exchange transfusion or had abnormal ABRs at discharge<sup>(13)</sup> and 8 full-term newborns (weight range 2.6-4.2 kg) with severe idiopathic hyperbilirubinemia ( $B_T$  28-34 mg/dL; 479-581  $\mu\text{mol/L}$ ).<sup>(19)</sup>

## PHOTOTHERAPY AND LIGHT DOSE

Two different systems were designed and constructed using affordable and commercially available materials to provide high-irradiance light therapy in the outpatient setting. The mainstay of phototherapy was a panel of ten 4-foot, 40W special Billi Blue (BB) fluorescent tubes (Phillips, Amsterdam, Netherlands) housed in a rigid, overhead, aluminum frame ( $66 \times 137$  cm).<sup>(17)</sup> The fully assembled unit weighed 18.2 kg. Newborns received 15-20 hours of phototherapy daily with 60%-70% of body surface exposed and light positioned 30-45 cm from the skin. For older children and adults, the light source was typically placed 45-60 cm from the skin and delivered at night to 35%-50% of skin surface. Mirrors were placed at the sides and head of the bed (Supporting Fig. S1). Patients used white sheets and did not shield their eyes.

More recently, 2 *UGT1A1* c.222C>A homozygotes were treated with a custom array of high-intensity light-emitting diodes (LEDs), designed and produced by HJV. The LED system consisted of an assembly of up to five aluminum panels, each with its own power cord, fused power inlet, and switch. A modular design allowed the number of panels to be adjusted to patient size (Fig. S1). Individual panels were mounted and joined along a central 3/4-inch sectional electrical conduit tube to yield a continuous therapeutic array plugged into a standard 110V or 220V AC power outlet. Individual panels were fitted with five 2-foot, 20W blue T8 LED tubes (Grandol Industry, Ltd., Shen Zhen, China), each with nine LEDs (i.e., 45 LEDs per panel) spaced 6 cm apart and emitting a peak wave-length of 468 (spectral range 415-536) nm. Single panels measured  $32 \times 61$  cm and weighed 1.81 kg; the entire five-panel system (25 LED tubes, 225 individual LEDs) measured  $168 \times 61$  cm, weighed 11.5 kg, and could be deconstructed and packed for transport into a  $71 \times 48 \times 30$  cm wheeled suitcase.

Daily light dose (W per hour/nm) is the product of irradiance ( $\mu\text{W}/\text{cm}^2$  per nm), body surface area exposed ( $\text{cm}^2$ ), and exposure time (hours). All irradiance measurements were taken with the BiliBlanket Meter II (GE Healthcare, Chicago, IL). The proportion of skin exposed to light is relatively fixed as a function of age. Thus, in practice, the two most relevant variables affecting light dose are skin-level irradiance and exposure time, which were titrated to maintain  $B_T/A < 0.7$  mol: mol; this value is 30% below the intravascular binding capacity (i.e.,  $B_T/A$  1.0 mol: mol), maintains  $B_f$  below its aqueous solubility limit,<sup>(6)</sup> and has proven to be well-tolerated by humans in the absence of ligands that compete for albumin binding.<sup>(13,17,19,20)</sup>

## LIVER FIBROSIS SCORE

Tissue from a liver biopsy or explant was available for 15 *UGT1A1* c.222C>A homozygotes. For each tissue sample, a weighted liver fibrosis score ( $L_f$ ) was calculated using the following equation:

$$L_f = 5[(F_c / 4) + (F_p / 6)], \quad (4)$$

where  $F_c$  is the central fibrosis score (range 0-4),  $F_p$  is the portal (Ishak) fibrosis score (range 0-6), and the weighted  $L_f$  score ranges from 0 (no fibrosis) to 10 (severe fibrosis).

## STATISTICS

Statistical calculations were done in Prism 8 (GraphPad, La Jolla, CA). Perinatal neurological risk factor data ( $B_T$ ,  $B_{T/A}$ , and days to phototherapy) were not normally distributed and were therefore analyzed using the two-tailed Mann-Whitney U test for unpaired observations. Normally distributed continuous variables were compared using the unpaired  $t$  test with Welch's correction (which does not assume equal variances). Associations between paired variables were tested using Pearson coefficients ( $r$ ) or simple linear correlation. Relationships of  $B_f$  to  $B_T$  and  $B_{T/A}$  were fit to an exponential model. Groups of three or more were compared using one-way analysis of variance (ANOVA) followed by the Tukey's *post hoc* test for pairwise comparisons. Kaplan-Meier analysis was applied to outcomes of kernicterus, liver transplantation, and survival. Standard contingency tables were constructed to calculate the sensitivity, specificity, positive predictive value (PPV), and likelihood ratio for disease (LRD).

## Results

### BILIRUBIN BINDING AND TISSUE DISTRIBUTION

We used sera from 7 healthy Amish controls, 18 *UGT1A1* c.222C>A homozygotes, 8 term newborns with idiopathic jaundice,<sup>(19)</sup> and 6 preterm infants weighing less than 1 kg<sup>(13)</sup> to examine the relationship among  $B_T$ ,  $A$ ,  $B_f$ , and  $K$  (Eq. 3) within  $B_T$  concentrations of 1.5-34.2 mg/dL (25-585  $\mu$ mol/L) and  $B_{T/A}$  values of 0.03-1.29 mol:mol (Table 2). As predicted by the mass action equation,  $B_f$  had a strong nonlinear relationship to both  $B_T$  ( $R^2 = 0.71$ ) and  $B_{T/A}$  ( $R^2 = 0.76$ ), and the proportion of  $B_T$  represented by  $B_f$  decreased exponentially with increasing values of  $K$  ( $R^2 = 0.69$ ) (Fig. 2).

At any given value of  $B_T$ , the serum albumin concentration and bilirubin-albumin equilibrium association binding constant are the main determinants of  $B_f$ . *UGT1A1* c.222C>A homozygotes as compared with jaundiced term newborns had similar albumin concentrations ( $4.4 \pm 0.5$  vs.  $3.9 \pm 0.6$  g/dL) and calculated values of  $K$  ( $118 \pm 57$  vs.  $101 \pm 36$  L/ $\mu$ mol) (Table 2); in both groups,  $B_f$  represented 0.001%-0.009% of  $B_T$ . Unbound bilirubin was proportionally highest (0.006%-0.025% of  $B_T$ ) in preterm babies less than 1 kg, who had the lowest levels of both albumin ( $3.0 \pm 0.8$  g/dL) and  $K$  ( $28 \pm 17$  L/ $\mu$ mol) (ANOVA  $P < 0.0001$ ) (Table 2, Fig. 2).

## KERNICTERUS: RISK FACTORS AND TIMING

In phototherapy-naïve newborns with CN1,  $B_T$  increased  $4.3 \pm 1.1$  (range 2.2-6.0) mg/dL per day to reach potentially neurotoxic concentrations by 5-14 days of age. This extrapolates to an endogenous bilirubin formation rate of  $3.7 \pm 0.9$  (range 1.9-5.1) mg/kg per day, remarkably close to the value of  $3.8 \pm 0.6$  mg/kg per day measured in healthy adults.<sup>(4)</sup> Four (14%) babies developed kernicterus between 14 and 45 days of age with presenting  $B_T$  and  $B_T/A$  values of 30-48 mg/dL (513-821  $\mu\text{mol/L}$ ) and 1.10-1.34 mol:mol, respectively (Fig. 2). All suffered permanent sequelae, including dystonia-chorea ( $n = 4$ ), dysphagia ( $n = 4$ ), mutism ( $n = 4$ ), hearing impairment ( $n = 2$ ), electrocortical abnormalities ( $n = 2$ ), and cerebral atrophy ( $n = 1$ ); 1 died of pneumonia at the age of 17 years.

Infants who did not develop kernicterus had lower presenting  $B_T$  (mean  $19.3 \pm 5.6$ , range 9.0-31.3 mg/dL;  $P = 0.001$ ) and  $B_T/A$  (mean  $0.59 \pm 0.20$ , range 0.25-1.07 mol:mol;  $P = 0.0005$ ) values, and started phototherapy at a median of 4 (range 1-27) as compared to 37 (range 14-91) days of age ( $P = 0.0007$ ). A presenting  $B_T$  of at least 30 mg/dL (513  $\mu\text{mol/L}$ ) or  $B_T/A$  of at least 1.0 mol:mol were equally predictive of kernicterus (sensitivity 100%, specificity 93.3%, PPV 80%, LRD 14), and babies who started phototherapy after the age of 13 days were 3.5 times more likely to sustain brain injury (Supporting Table S2, Fig. 2).

One additional patient suffered a fatal neurological crisis during early childhood. He was developing normally, with  $B_T$  concentrations ranging from 15 to 25 mg/dL on 7-12 hours of phototherapy daily. At 7 years of age, he presented to an urgent care center with *Streptococcal* pharyngitis and was prescribed amoxicillin for outpatient treatment. The following day, his speech deteriorated and he stopped eating. Four days later, he presented to a regional Midwestern hospital febrile, lethargic, ataxic, and mute. Presenting laboratory studies showed  $B_T = 39$  mg/dL (667  $\mu\text{mol/L}$ ), albumin = 2.9 g/dL (441  $\mu\text{mol/L}$ ), and  $B_T/A = 1.52$  mol:mol. An electroencephalogram revealed diffuse slowing and generalized paroxysmal spikes. Magnetic resonance imaging of the brain was normal. He was managed with continuous phototherapy, intravenous crystalloid, albumin, and phenobarbital. His  $B_T$  decreased to baseline but neurological function did not improve. He died a few weeks later.

## HYPERBILIRUBINEMIA AND PHOTOTHERAPY

Following the perinatal period, light was delivered  $9.2 \pm 1.1$  (range 7.0-12.5) hours daily to maintain an average  $B_T$  of  $17.0 \pm 5.9$  (range 3.7-38.7) mg/dL and  $B_T/A$  of  $0.47 \pm 0.17$  (range 0.10-1.51) mol:mol (Table 3). The serum  $B_T/Alb$  ratio was lower ( $0.49 \pm 0.15$  vs.  $0.44 \pm 0.09$ ,  $P = 0.0009$ ) and less variable ( $F = 3.02$ ,  $P < 0.0001$ ) in patients treated with LED as compared with BB fluorescent lights (Fig. 3). Irradiance decayed with distance from both light sources ( $r^2 = 0.98$ ,  $P < 0.0001$ ). LED arrays were 44%-109% more powerful than BB fluorescent tubes ( $89 \pm 10$  [ $13 \mu\text{W/cm}^2$  per nm vs.  $52 \pm 13 \mu\text{W/cm}^2$  per nm;  $P < 0.0001$ ]) within clinically relevant operating distances of 30-60 cm from the skin. Despite relatively uniform phototherapy conditions,  $B_T$  and  $B_T/A$  increased an average of 0.46 mg/dL and 0.013 mol:mol per year ( $r^2 = 0.21$ ;  $P < 0.0001$ ), respectively, and by 18 years of age reached potentially dangerous values (75%-95% saturation of intravascular binding capacity) (Fig. 3).

Phototherapy restricted social opportunities and travel but had no serious adverse effects. As previously reported<sup>(17)</sup> 5 *UGT1A1* c.222C>A homozygotes exposed to 100,000 or more hours of phototherapy with unshielded eyes had normal visual acuity and color discrimination as compared with their age-matched siblings. Several fair-complected patients developed chronic dyspigmentation of light-exposed skin, but this required no specific intervention. No member of the cohort developed light-induced erythema or skin cancer.

## CHOLELITHIASIS AND CHRONIC HEPATOPATHY

Twelve (43%) of the 28 *UGT1A1* c.222C>A homozygotes were diagnosed with cholelithiasis, most often presenting with abdominal pain and exacerbation of hyperbilirubinemia. All underwent cholecystectomy, which revealed numerous small pigmentary stones.

Liver tissue was available from 15 (56%) of 27 *UGT1A1* c.222C>A homozygotes (median age 14.6 years, range 4.4-23.6 years). Most tissue sections showed intrahepatic cholestasis and nine (60%) livers had fibrosis ranging from mild to severe (Fig. 4). The degree of fibrosis, as determined by a central–portal weighted fibrosis score ( $L_f$ ; Eq. 4), correlated with the lifetime average  $B_T$  ( $r = 0.60$ ,  $P < 0.0023$ ; mean 32 values per patient). Using longitudinal data from all 28 *UGT1A1* homozygotes ( $n = 416$  paired values), we found a correlation between simultaneously collected  $B_T$  and alanine aminotransferase concentrations ( $r = 0.24$ ;  $P < 0.0001$ ).

## LIVER TRANSPLANTATION

Seventeen (63%) *UGT1A1* c.222C>A homozygotes received an orthotopic liver transplant at a median age of 16.2 (range 4.7-23.2) years (Fig. 4). Fifteen allografts were from deceased unrelated donors; 2 patients were successfully “domino” grafted from living donors homozygous for *BCKDHA* c.1312T>A, undergoing liver transplantation for treatment of classical maple syrup urine disease<sup>(21)</sup> Serum  $B_T$  decreased precipitously within days after transplant and remained stable thereafter. Based on 113 samples from 17 individuals, the mean posttransplant  $B_T$  was  $0.8 \pm 0.5$  (range 0.1-3.5) mg/dL (Table 3). One transplanted patient died from unrelated circumstances. Sixteen remaining patients are alive and well, with posttransplant graft and patient survival of 100% over 0.1-14.9 (median 7.6) years of follow-up.

## Discussion

### BILIRUBIN BIODISTRIBUTION AND TISSUE LOADING

The distribution of unconjugated bilirubin between intravascular and extravascular compartments is a critical determinant of potential toxicity that depends on the interaction between bilirubin and albumin. In CN1 patients, the bilirubin–albumin complex behaves as predicted (Eq. 3), and the correlation between  $B_f$  and  $B_T/A$  is governed by an average equilibrium association binding constant ( $118 \pm 57$  L/ $\mu$ mol) remarkably close to that observed in term newborns ( $101 \pm 36$  L/ $\mu$ mol). This allows  $B_T/A$  to serve as a surrogate for  $B_f$ . Using aggregate longitudinal data for all CN1 patients,  $B_T/A \approx 1.0$  mol:mol (PPV



83.3%; LRD 473; n = 481) is superior to  $B_T > 30$  mg/dL (PPV 35.7%; LRD 70; n = 646) as an index of neurological risk, but provides no predictive advantage over  $B_T$  alone in newborns (Supporting Table S1).<sup>(20)</sup>

The coefficient of variation for K between individuals ranges from 36% (term newborns) to 60% (preterm). Such variability can account for 10-fold differences in  $B_f$  at any given  $B_T/A$  (Fig. 3) and ultimately limits the predictive value of both  $B_T$  and  $B_T/A$  across clinical populations. Albumin and K values are especially low in preterm babies (Table 2), explaining why  $B_T$  levels as low as 8.5 mg/dL (145  $\mu$ mol/L) can cause kernicterus in this vulnerable group. Predicting the relationship among  $B_T$ ,  $B_f$ , and kernicterus is further complicated by an unquantified element of tissue exposure. As bilirubin circulates through the brain, some proportion is continually “stripped” from albumin by cerebral membranes.<sup>(22)</sup> For any particular set of  $B_T$ ,  $B_T/A$ , and  $B_f$  values, more pigment deposits in the brain when cerebral blood flow is high, bilirubin dissociates rapidly from albumin, or blood moves slowly through tissue capillaries.

In experimental animals, cerebral bilirubin uptake is typically 30%-50% lower than predicted by mathematical models.<sup>(22)</sup> One reason for this discrepancy is extrusion of bilirubin by adenosine triphosphate–dependent drug efflux pumps expressed at the blood–brain barrier (e.g., ABCB1 [i.e., P-glycoprotein, MDR1]),<sup>(23)</sup> a capacity that is low in newborn brain,<sup>(24)</sup> matures postnatally,<sup>(25)</sup> and may adapt to chronic bilirubin exposure.<sup>(26)</sup> In CN1 patients exposed to high  $B_T$  concentrations for decades, the ability of cerebral endothelia to extrude bilirubin back to the intravascular space might safeguard the brain against chronic toxicity. This underscores the primacy of tissue bilirubin load, not its intravascular concentration, as the ultimate determinant of neuronal injury (Fig. 2). Unfortunately, the former cannot be measured *in vivo*.

## RISK FACTORS FOR KERNICTERUS

In newborns with CN1, the kinetics of postnatal bilirubin tissue loading is relatively predictable (Fig. 2):  $B_T$  increases  $4.3 \pm 1.1$  (range 2.2-6.0) mg/dL per day to saturate intravascular binding capacity between 5 and 10 postnatal days of age; thereafter, blood albumin concentration sets an upper limit on *measured*  $B_T$  concentration as unmeasured pigment continues to accumulate in the brain and other tissues.<sup>(1,13)</sup> Knowledge of the *UGT1A1* c.222C>A founder allele allows us to anticipate tissue bilirubin loading in high-risk newborns (Table 4), but this advantage is offset by socioeconomic challenges. Most Plain families are uninsured, live in rural areas, and deliver their children at home. Some affected neonates are not seen by a physician for several postnatal weeks, during which jaundice is monitored by the unreliable practice of visual inspection.<sup>(27)</sup> Thus, within our cohort, each case of perinatal kernicterus befell unsuspecting parents and could have been prevented by systematic bilirubin screening within the first week of life.<sup>(28)</sup>

Intercurrent illness represents a special threat to CN1 patients of all ages, as vividly illustrated by a fatal case of kernicterus in a 7-year-old boy. While infected with *Streptococcus*, his  $B_T$  increased 2-fold, albumin decreased 30%, and the  $B_T/A$  ratio increased from 0.50 to 1.52 mol:mol. Under such conditions, a  $B_T$  of only 23 mg/dL (390  $\mu$ mol/L) is sufficient to saturate intravascular binding and increase  $B_f$  to its aqueous

solubility limit. At the measured  $B_T$  of 39 mg/dL (438  $\mu\text{mol/L}$ ),  $B_f$  was likely supersaturated in plasma, driving massive pigment deposition in the brain.<sup>(19)</sup>

Such biochemical changes associated with the normal acute phase response can be catastrophic in patients with CN1. Inflammatory states are characterized by shortened erythrocyte survival, contraction of plasma volume, and reduced enteral intake (which decreases enterohepatic flow; Fig. 1), all of which increase circulating  $B_T$ . Albumin is a “negative” acute phase protein, decreasing 10%-40% in response to diverse inflammatory stimuli.<sup>(29)</sup> Thus, during infectious illnesses, CN1 patients commonly experience a 25%-50% increase of  $B_T$  accompanied by hypoalbuminemia.

In hospitalized patients with severe hyperbilirubinemia, we treat hypoalbuminemia with intravenous albumin infusions (1-2 g/kg per dose up to every 6 hours) (Table 1). In principle, each gram of albumin per kilogram of body weight should increase the plasma concentration about 1.25 g/dL (assuming a circulating blood volume of 80 mL/kg). The observed increase is consistently lower, likely reflecting some albumin escape into the extravascular space as well as expansion of plasma volume driven by oncotic pressure. In the clinical setting, each albumin infusion reliably decreases  $B_T/A$  by 10%-20%, but is commonly followed by a transient *increase* of  $B_T$  caused by redistribution of tissue-bound pigment to intravascular binding sites.

Certain drugs and exogenous ligands administered during illness also have the potential to precipitate kernicterus. This was first dramatically demonstrated in 1956, when 193 low-birth-weight infants were randomly assigned to receive antibacterial prophylaxis with either oxytetracycline or penicillin-sulfisoxazole.<sup>(30)</sup> Mortality was more than 2-fold higher in the latter group, attributable not to infections but to a higher incidence of kernicterus observed in postmortem tissue (43.2% vs. 4.5%). Experimental studies subsequently showed that sulfisoxazole competitively displaces bilirubin from intravascular to extravascular sites,<sup>(31)</sup> and when administered to jaundiced Gunn rats, decreases intravascular  $B_T$ , exacerbates cerebral staining, and increases mortality.<sup>(32)</sup> A number of exogenous ligands (most notably antibiotics, drug preservatives, and intravenous contrast agents) interfere with bilirubin–albumin binding and can precipitate neurological injury in any jaundiced patient (Supporting Table S2).

## PHOTOTHERAPY

A variety of contemporary phototherapy systems provide high irradiance over a large body surface and, if properly used, afford CN1 patients long-term protection from neurological injury. To optimize phototherapy, any apparatus should be placed as close as tolerable to maximal skin surface (Fig. 3) and surrounded everywhere by white or reflective surfaces (Table 1, Supporting Fig. S1). All available systems that provide sufficient irradiance also generate heat, and patients with Crigler-Najjar often require active nocturnal cooling by electric fans or conditioned air. As previously reported,<sup>(17)</sup> fiber optic systems produce low irradiance compared with fluorescent BB and LED sources and are not appropriate for treatment of serious hyperbilirubinemia.

Commercial phototherapy systems are expensive and difficult to procure in resource-limited settings. The fluorescent BB unit can be constructed for under US \$500 in materials, generates irradiance values equal to or greater than most commercial systems,<sup>(17)</sup> and has been life-saving for patients with restricted access to medical technology. However, it is large, rigid, and heavy, and uses a light source that decays rapidly with use. Newer systems exploit the higher efficiency and irradiance of LEDs. The full-size (5-panel) LED phototherapy unit costs only about US \$1,000 in materials and allows better and tighter control of serum B<sub>T</sub> levels with lower overall system maintenance (Fig. 3). The LED system is also lighter, cooler, and features a modular design that enables size-matching and portability.

Our data reveal no serious health consequences for individuals exposed to more than 100,000 hours of high-intensity phototherapy over their lifetime. Phototherapy dependence primarily interferes with lifestyle and interpersonal relationships. All high-irradiance light units are cumbersome and require a dedicated power source, limiting opportunities for travel. As CN1 patients mature, nocturnal phototherapy is particularly obstructive to the formation of intimate relationships.

## LIVER TRANSPLANTATION

Transplantation of allogeneic liver tissue introduces nearly 100% functional enzyme activity on a whole-body basis, reduces B<sub>T</sub> into the normal range, and affords decisive protection from kernicterus. Because only 30% or less of hepatic UGT1A1 activity is required to maintain normal bilirubin homeostasis,<sup>(33)</sup> tissue segments from related (i.e., heterozygous) living donors are sufficient to correct hyperbilirubinemia.<sup>(34)</sup> Interestingly, 2 patients from our cohort were successfully domino grafted from *BCKDHA* c.1312T>A homozygotes who underwent liver transplantation for treatment of classical maple syrup urine disease (MSUD). This strategy works because of the large reservoir of branched-chain ketoacid dehydrogenase activity in muscle.<sup>(35)</sup>

Patients with Crigler-Najjar were in a larger cohort of 115 individuals transplanted between 1997 and the present for various metabolic indications (CN1, n = 17; MSUD, n = 93; progressive familial intrahepatic cholestasis type 1, n = 3; S-adenosylhomocysteine hydrolase deficiency, n = 1; GM3 synthase deficiency, n = 1) as part of a broader collaboration between CSC and UPMC Children's Hospital of Pittsburgh. Excluding 1 individual who died of unrelated causes, overall patient and graft survival were 100% and 99.1%, respectively, and rates of early postoperative complications (5%-34%) were similar to those reported by others.<sup>(36)</sup> Among published cases, the overall complication rate is higher (40%-83%) with partial auxiliary grafts, some of which atrophy over time.<sup>(37)</sup>

Progressive hepatopathy might ultimately necessitate liver transplantation or some other definitive intervention in most CN1 patients (Fig. 3). The causal relationship of hyperbilirubinemia to liver disease is not completely understood. Chronic cholangiopathy has been associated with hepatic fibrosis in other clinical settings,<sup>(38)</sup> whereas more recent data suggest that B<sub>T</sub> and/or higher-order heme degradation products might be cytotoxic to certain nonneuronal cells.<sup>(39)</sup> Two oxidation products (Z-BOX A and Z-BOX B) produced during heme degradation are about 20-fold elevated in serum of both hyperbilirubinemic

Gunn rats and humans with cholestasis.<sup>(40)</sup> In cultured hepatocytes, high concentrations of Z-BOX A and B differentially modulate two nuclear receptor transcription factors (NR1D1 and NR1D2), deplete cells of reduced glutathione, and activate cytoskeletal remodeling, indicating a potential role in the hepatopathy of CN1.

In conclusion, 67 years following its discovery, Crigler-Najjar syndrome remains a morbid and potentially fatal disorder (Table 4).<sup>(1,41-46)</sup> In developed nations, brain injury occurs in 18%-26% of patients with Crigler-Najjar, a figure that has remained essentially unchanged during the last 2 decades. Kernicterus rates are higher (50%-93%) in countries where medical resources are scarce and home phototherapy is difficult to procure. This same pattern of disparity applies to liver transplantation, which is only available to a small number of patients (0%-17%) who live in developing nations.

Although liver transplantation represents an effective form of “gene therapy” for CN1, it entails well-known surgical, infectious, and malignant risks. Emerging therapies hold promise. In transgenic animal models of CN1, repeated intravenous administration of *UGT1A1* mRNA rescues a lethal phenotype and normalizes plasma  $B_T$ , whereas a single injection of liver-specific adeno-associated virus (AAV) type 9 containing human *UGT1A1* controls  $B_T$  for life.<sup>(33,47)</sup> However, normal liver growth (e.g., from about 120 g to 1,400 g in humans) dilutes out nonreplicating transgenes delivered by AAV<sup>(48)</sup>; thus, genome editing might prove a more durable solution for very young patients.

## Supplementary Material

Refer to Web version on PubMed Central for supplementary material.

## Acknowledgments:

This paper is dedicated to Drs. John Fielding Crigler, Jr. (1919-2018) and Victor Assad Najjar (1914-2002) and the children and families we serve. The authors thank Dr. D. Holmes Morton for his invaluable contributions to the design and implementation of treatment strategies for CN1.

## Abbreviations:

<b>ANOVA</b>	analysis of variance
<b>BB</b>	Billi Blue
<b>CN1</b>	Crigler-Najjar type 1 syndrome
<b>CSC</b>	Clinic for Special Children
<b>LEDs</b>	light-emitting diodes
<b>LRD</b>	likelihood ratio for disease
<b>MW</b>	molecular weight
<b>PPV</b>	positive predictive value
<b>UGT1A1</b>	uridine 5'-diphosphate glucuronyltransferase

## REFERENCES

- 1). Crigler JF Jr., Najjar VA. Congenital familial nonhemolytic jaundice with kernicterus. *Pediatrics* 1952;10:169–180. [PubMed: 12983120]
- 2). Mackenzie PI, Owens IS, Burchell B, Bock KW, Bairoch A, Belanger A, et al. The UDP glycosyltransferase gene superfamily: recommended nomenclature update based on evolutionary divergence. *Pharmacogenetics* 1997;7:255–269. [PubMed: 9295054]
- 3). Brodersen R, Tygstrup N. Specific determination of serum bilirubin diglucuronide in patients with hepato-biliary diseases. *Scand J Clin Lab Invest* 1969;23:55–58. [PubMed: 5363435]
- 4). Berk PD, Howe RB, Bloomer JR, Berlin NI. Studies of bilirubin kinetics in normal adults. *J Clin Invest* 1969;48:2176–2190. [PubMed: 5824077]
- 5). Brodersen R, Stern L. Deposition of bilirubin acid in the central nervous system—a hypothesis for the development of kernicterus. *Acta Paediatr Scand* 1990;79:12–19. [PubMed: 2180252]
- 6). Wennberg RP, Ahlfors CE, Rasmussen LF. The pathochemistry of kernicterus. *Early Hum Dev* 1979;3:353–372. [PubMed: 43803]
- 7). Jacobsen J, Brodersen R. Albumin-bilirubin binding mechanism. *J Biol Chem* 1983;258:6319–6326. [PubMed: 6853485]
- 8). Wennberg RP. The blood-brain barrier and bilirubin encephalopathy. *Cell Mol Neurobiol* 2000;20:97–109. [PubMed: 10690504]
- 9). Katoh-Semba R, Kashiwamata S. Interaction of bilirubin with brain capillaries and its toxicity. *Biochim Biophys Acta* 1980;632:290–297. [PubMed: 7417528]
- 10). Roger C, Koziel V, Vert P, Nehlig A. Mapping of the consequences of bilirubin exposure in the immature rat: local cerebral metabolic rates for glucose during moderate and severe hyperbilirubinemia. *Early Hum Dev* 1995;43:133–144. [PubMed: 8903758]
- 11). Waters WJ. The protective action of albumin in bilirubin toxicity in newborn puppies. In: Sass-Kortsak A, ed. *Kernicterus*. Toronto: University of Toronto Press; 1961:219–221.
- 12). Ahlfors CE, Amin SB, Parker AE. Unbound bilirubin predicts abnormal automated auditory brainstem response in a diverse newborn population. *J Perinatol* 2009;29:305–309. [PubMed: 19242487]
- 13). Ahlfors CE, Wennberg RP, Ostrow JD, Tiribelli C. Unbound (free) bilirubin: improving the paradigm for evaluating neonatal jaundice. *Clin Chem* 2009;55:1288–1299. [PubMed: 19423734]
- 14). Stern L, Brodersen R. Kernicterus research and the basic sciences: a prospect for future development. *Pediatrics* 1987;79:154–156. [PubMed: 3797160]
- 15). Lucey J, Ferriero M, Hewitt J. Prevention of hyperbilirubinemia of prematurity by phototherapy. *Pediatrics* 1968;41:1047–1054. [PubMed: 5652916]
- 16). Cremer RJ, Perryman PW, Richards DH. Influence of light on the hyperbilirubinaemia of infants. *Lancet* 1958;1:1094–1097. [PubMed: 13550936]
- 17). Strauss KA, Robinson DL, Vreman HJ, Puffenberger EG, Hart G, Morton DH. Management of hyperbilirubinemia and prevention of kernicterus in 20 patients with Crigler-Najjar disease. *Eur J Pediatr* 2006;165:306–319. [PubMed: 16435131]
- 18). Ahlfors CE. Effect of serum dilution on apparent unbound bilirubin concentration as measured by the peroxidase method. *Clin Chem* 1981;27:692–696. [PubMed: 7226493]
- 19). Ahlfors CE, Herbsman O. Unbound bilirubin in a term newborn with kernicterus. *Pediatrics* 2003;111:1110–1112. [PubMed: 12728100]
- 20). Iskander I, Gamaleldin R, El Houchi S, El Shenawy A, Seoud I, El Gharbawi N, et al. Serum bilirubin and bilirubin/albumin ratio as predictors of bilirubin encephalopathy. *Pediatrics* 2014;134:e1330–e1339. [PubMed: 25332491]
- 21). Khanna A, Hart M, Nyhan WL, Hassanein T, Panyard-Davis J, Barshop BA. Domino liver transplantation in maple syrup urine disease. *Liver Transpl* 2006;12:876–882. [PubMed: 16628687]
- 22). Robinson PJ, Rapoport SI. Binding effect of albumin on uptake of bilirubin by brain. *Pediatrics* 1987;79:553–558. [PubMed: 3822673]

- 23). Bockor L, Bortolussi G, Vodret S, Iaconcig A, Jasprova J, Zelenka J, et al. Modulation of bilirubin neurotoxicity by the Abcb1 transporter in the Ugt1<sup>-/-</sup> lethal mouse model of neonatal hyperbilirubinemia. *Hum Mol Genet* 2017;26:145–157. [PubMed: 28025333]
- 24). Lam J, Baello S, Iqbal M, Kelly LE, Shannon PT, Chitayat D, et al. The ontogeny of P-glycoprotein in the developing human blood-brain barrier: implication for opioid toxicity in neonates. *Pediatr Res* 2015;78:417–421. [PubMed: 26086643]
- 25). Daood M, Tsai C, Ahdab-Barmada M, Watchko JF. ABC transporter (P-gp/ABCB1, MRP1/ABCC1, BCRP/ABCG2) expression in the developing human CNS. *Neuropediatrics* 2008;39:211–218. [PubMed: 19165709]
- 26). Gazzin S, Berengeno AL, Strazielle N, Fazzari F, Raseni A, Ostrow JD, et al. Modulation of Mrp1 (ABCC1) and Pgp (ABCB1) by bilirubin at the blood-CSF and blood-brain barriers in the Gunn rat. *PLoS One* 2011;6:e16165. [PubMed: 21297965]
- 27). Moyer VA, Ahn C, Sneed S. Accuracy of clinical judgment in neonatal jaundice. *Arch Pediatr Adolesc Med* 2000;154: 391–394. [PubMed: 10768679]
- 28). Bhutani VK, Johnson LH, Jeffrey Maisels M, Newman TB, Phibbs C, Stark AR, et al. Kernicterus: epidemiological strategies for its prevention through systems-based approaches. *J Perinatol* 2004;24:650–662. [PubMed: 15254556]
- 29). Liao WS, Jefferson LS, Taylor JM. Changes in plasma albumin concentration, synthesis rate, and mRNA level during acute inflammation. *Am J Physiol* 1986;251:C928–C934. [PubMed: 3789133]
- 30). Andersen DH, Blanc WA, Crozier DN, Silverman WA. A difference in mortality rate and incidence of kernicterus among premature infants allotted to two prophylactic antibacterial regimens. *Pediatrics* 1956;18:614–625. [PubMed: 13370229]
- 31). Odell GB. The dissociation of bilirubin from albumin and its clinical implications. *J Pediatr* 1959;55:268–279. [PubMed: 14428276]
- 32). Blanc WA, Johnson L. Studies on kernicterus; relationship with sulfonamide intoxication, report on kernicterus in rats with glucuronyl transferase deficiency and review of pathogenesis. *J Neuropathol Exp Neurol* 1959;18:165–189; discussion 187–169. [PubMed: 13621251]
- 33). Bortolussi G, Zentillin L, Vanikova J, Bockor L, Bellarosa C, Mancarella A, et al. Life-long correction of hyperbilirubinemia with a neonatal liver-specific AAV-mediated gene transfer in a lethal mouse model of Crigler-Najjar Syndrome. *Hum Gene Ther* 2014;25:844–855. [PubMed: 25072305]
- 34). Ozcay F, Alehan F, Sevmis S, Karakayali H, Moray G, Torgay A, et al. Living related liver transplantation in Crigler-Najjar syndrome type I. *Transplant Proc* 2009;41:2875–2877. [PubMed: 19765461]
- 35). Mazariegos GV, Morton DH, Sindhi R, Soltys K, Nayyar N, Bond G, et al. Liver transplantation for classical maple syrup urine disease: long-term follow-up in 37 patients and comparative United Network for Organ Sharing experience. *J Pediatr* 2012;160:116–121, e111. [PubMed: 21839471]
- 36). Pett S, Mowat AP. Crigler-Najjar syndrome types I and II. Clinical experience—King's College Hospital 1972–1978. Phenobarbitone, phototherapy and liver transplantation. *Mol Aspects Med* 1987;9:473–482. [PubMed: 3306242]
- 37). Rela M, Muiesan P, Vilca-Melendez H, Dhawan A, Baker A, Mieli-Vergani G, et al. Auxiliary partial orthotopic liver transplantation for Crigler-Najjar syndrome type I. *Ann Surg* 1999;229:565–569. [PubMed: 10203091]
- 38). Mitchell E, Ranganathan S, McKiernan P, Squires RH, Strauss K, Soltys K, et al. Hepatic parenchymal injury in Crigler-Najjar type I. *J Pediatr Gastroenterol Nutr* 2018;66:588–594. [PubMed: 29176474]
- 39). Elias MM, Comin EJ, Grosman ME, Galeazzi SA, Rodriguez Garay EA. Possible mechanism of unconjugated bilirubin toxicity on renal tissue. *Comp Biochem Physiol A Comp Physiol* 1987;87:1003–1007. [PubMed: 2887366]
- 40). Seidel RA, Claudel T, Schleser FA, Ojha NK, Westerhausen M, Nietzsche S, et al. Impact of higher-order heme degradation products on hepatic function and hemodynamics. *J Hepatol* 2017;67:272–281. [PubMed: 28412296]

- 41). van der Veere CN, Sinaasappel M, McDonagh AF, Rosenthal P, Labrune P, Odievre M, et al. Current therapy for Crigler-Najjar syndrome type 1: report of a world registry. *Hepatology* 1996;24:311–315. [PubMed: 8690398]
- 42). Lucey JF, Suresh GK, Kappas A. Crigler-Najjar syndrome, 1952–2000: learning from parents and patients about a very rare disease and using the internet to recruit patients for studies. *Pediatrics* 2000;105:1152–1153. [PubMed: 10790478]
- 43). Suresh G, Lucey JF. Lack of deafness in Crigler-Najjar syndrome type 1: a patient survey. *Pediatrics* 1997;100:E9.
- 44). Shevell MI, Majnemer A, Schiff D. Neurologic perspectives of Crigler-Najjar syndrome type I. *J Child Neurol* 1998;13:265–269. [PubMed: 9660509]
- 45). Nazer H, Al-Mehaidib A, Shabib S, Ali MA. Crigler-Najjar syndrome in Saudi Arabia. *Am J Med Genet* 1998;79: 12–15. [PubMed: 9738861]
- 46). Aloulou H, Ben Thabet A, Khanfir S, Ben Mansour L, Chabchoub I, Labrune P, et al. Type I Crigler Najjar syndrome in Tunisia: a study of 30 cases. *Tunis Med* 2010;88:707–709. [PubMed: 20890816]
- 47). Apgar JF, Tang JP, Singh P, Balasubramanian N, Burke J, Hodges MR, et al. Quantitative Systems Pharmacology Model of hUG-T1A1-modRNA encoding for the UGT1A1 enzyme to treat Crigler-Najjar Syndrome type 1. *CPT Pharmacometrics Syst Pharmacol* 2018;7:404–412. [PubMed: 29637732]
- 48). Villiger L, Grisch-Chan HM, Lindsay H, Ringnalda F, Pogliano CB, Allegri G, et al. Treatment of a metabolic liver disease by in vivo genome base editing in adult mice. *Nat Med* 2018;24:1519–1525. [PubMed: 30297904]

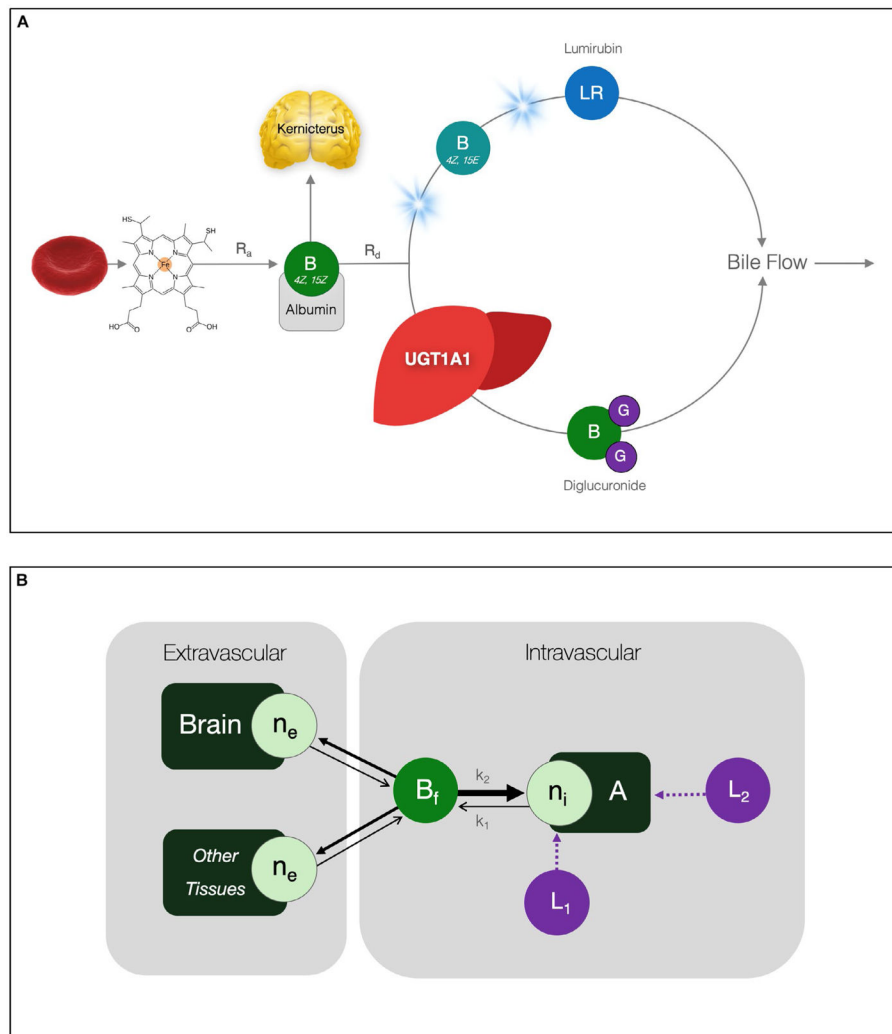


**FIG. 1.** Bilirubin metabolism and biodistribution. (A) Native 4Z,15Z-bilirubin is a degradation product of heme derived primarily from senescent erythrocytes. Its rate of appearance ( $R_a$ ) is governed by the kinetics of red cell destruction. Under normal conditions, hepatocyte UGT1A1 adds glucuronides to native bilirubin and water-soluble diglucuronide enters bile canaliculi for excretion. Bilirubin elimination from the body ( $R_d$ ) depends on hepatic UGT1A1 activity, diglucuronide transport into canaliculi, and total bile flow. Illumination of bilirubin with 430-490 nm (“blue”) spectrum light reversibly converts 4Z,15Z-bilirubin to its 4Z,15E isomer, a portion of which further isomerizes to lumirubin, the chemically stable phototherapy product that predominates in bile. (B) Unbound (“free”) bilirubin ( $B_f$ ) is the neurotoxic fraction; it has low aqueous solubility ( $\sim 70$  nmol/L;  $4$   $\mu\text{g}/\text{dL}$ ) and moves in chemical equilibria between a finite number of intravascular binding sites ( $n_i$ ) on albumin (A) and a larger number of low-affinity extravascular sites ( $n_e$ ) in brain and other tissues. The values of  $k_1$  ( $\text{sec}^{-1}$ ) and  $k_2$  ( $\mu\text{mol}/\text{L}$  per second) represent the dissociation and association rate constants, respectively, and  $k_1/k_2$  is  $K$  ( $\text{L}/\mu\text{mol}$ ), the bilirubin–albumin equilibrium association binding constant. Various ligands (e.g., antibiotics) interfere with



binding by either competing directly for the bilirubin binding site ( $L_1$ ) or indirectly altering its association constant ( $L_2$ ). Abbreviation: LR, lumirubin.

Author Manuscript

Author Manuscript

Author Manuscript

Author Manuscript

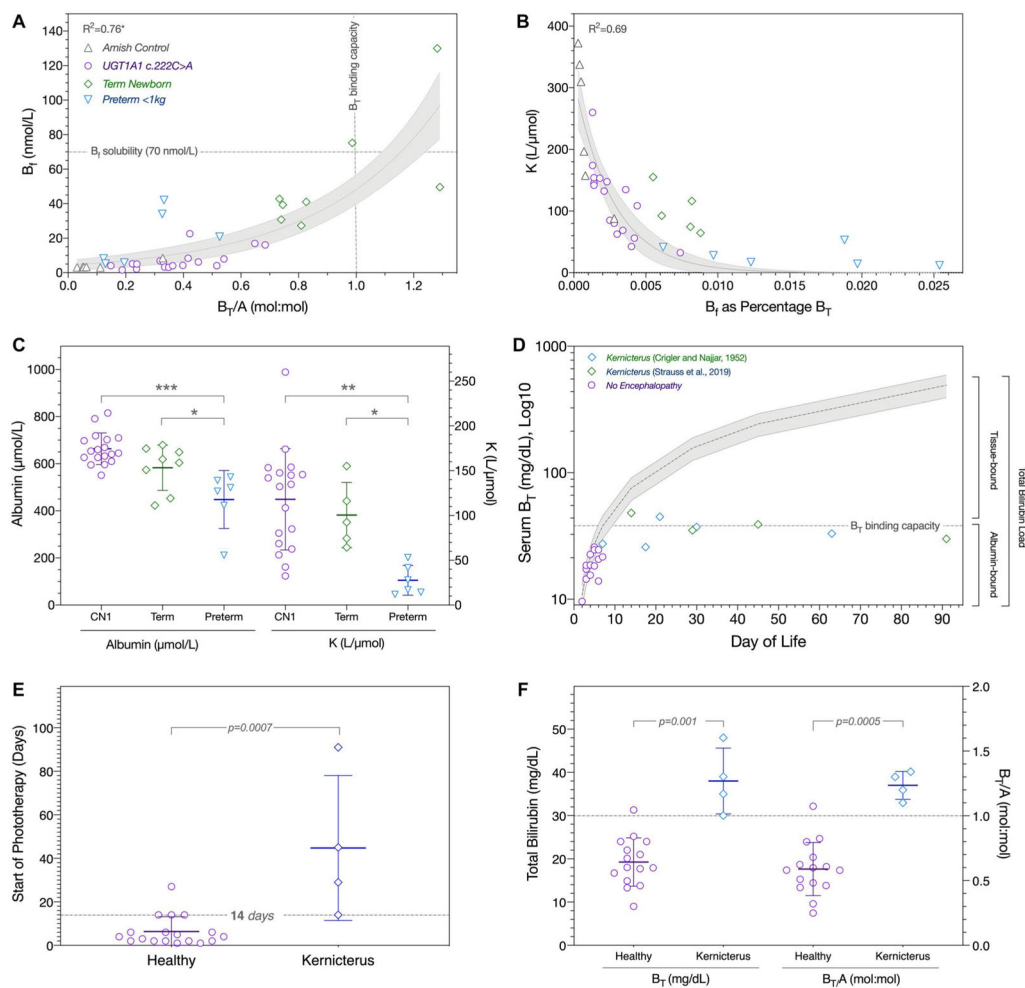


**FIG. 2.**

Bilirubin–albumin binding, tissue loading, and kernicterus. (A) Gray horizontal and vertical lines indicate  $B_f$  aqueous solubility and intravascular  $B_T$  binding capacity, respectively. There is an exponential relationship between  $B_f$  and  $B_T/A$  ( $R^2 = 0.76$ ; 95% confidence interval shaded gray) (Amish controls, gray triangles; *UGT1A1 c.222C>A* homozygotes, purple circles; term newborns with idiopathic jaundice, green diamonds; preterm infants weighing less than 1 kg, blue triangles). (B) The proportion of  $B_T$  represented by  $B_f$  decreases exponentially with increasing values of  $K$  ( $R^2 = 0.69$ ). (C) *UGT1A1 c.222C>A* homozygotes (CN1) as compared with jaundiced term newborns had similar albumin concentrations (left y-axis) and calculated values of  $K$  (right y-axis), whereas preterm babies weighing less than 1 kg had the lowest levels of both albumin and  $K$  (ANOVA  $P < 0.0001$ ; Tukey's *post hoc* test:  $*P < 0.05$ ,  $**P < 0.01$ ,  $***P < 0.001$ ). (D)  $B_T$  values (log10 scale) are plotted for 5 patients originally described by Crigler and Najjar (green diamonds<sup>(1)</sup>), 4 neonates from the present cohort who developed kernicterus (blue diamonds), and 14 *UGT1A1 c.222C>A* homozygotes who escaped neurological injury (purple circles). Gray shading depicts the theoretical increase of  $B_T$  if produced at a steady rate of  $3.7 \pm 0.9$  mg/kg per day and confined to the circulation. Within a normal range of albumin concentrations (3.5 and 4.5 g/dL), intravascular binding capacity (horizontal dashed line) saturates between

5 and 10 days of age and sets an upper limit on the concentration of intravascular  $B_T$ . Thereafter, unmeasured pigment binds to brain and other extravascular tissues and comes to comprise 60%-90% of the total bilirubin load at the time of kernicterus. (E) Neonates who developed kernicterus (blue diamonds) started phototherapy at a median age of 37 postnatal days as compared with 4 postnatal days of age for those who remained healthy (purple circles); initiation of phototherapy at 14 or more postnatal days of age (gray line) increased the likelihood of brain injury 3.5 fold. (F) All 4 neonates who suffered brain injury had a  $B_T/A$  greater than 1.0 mol:mol between 15 and 45 postnatal days of age. The presenting  $B_T/A$  was about 60% lower among the 24 remaining infants who did not develop kernicterus. As predictors of kernicterus during the neonatal period,  $B_T > 30$  mg/dL or  $B_T/A > 1.0$  mol:mol had equal specificity (93.3%) and PPV (80.0%).

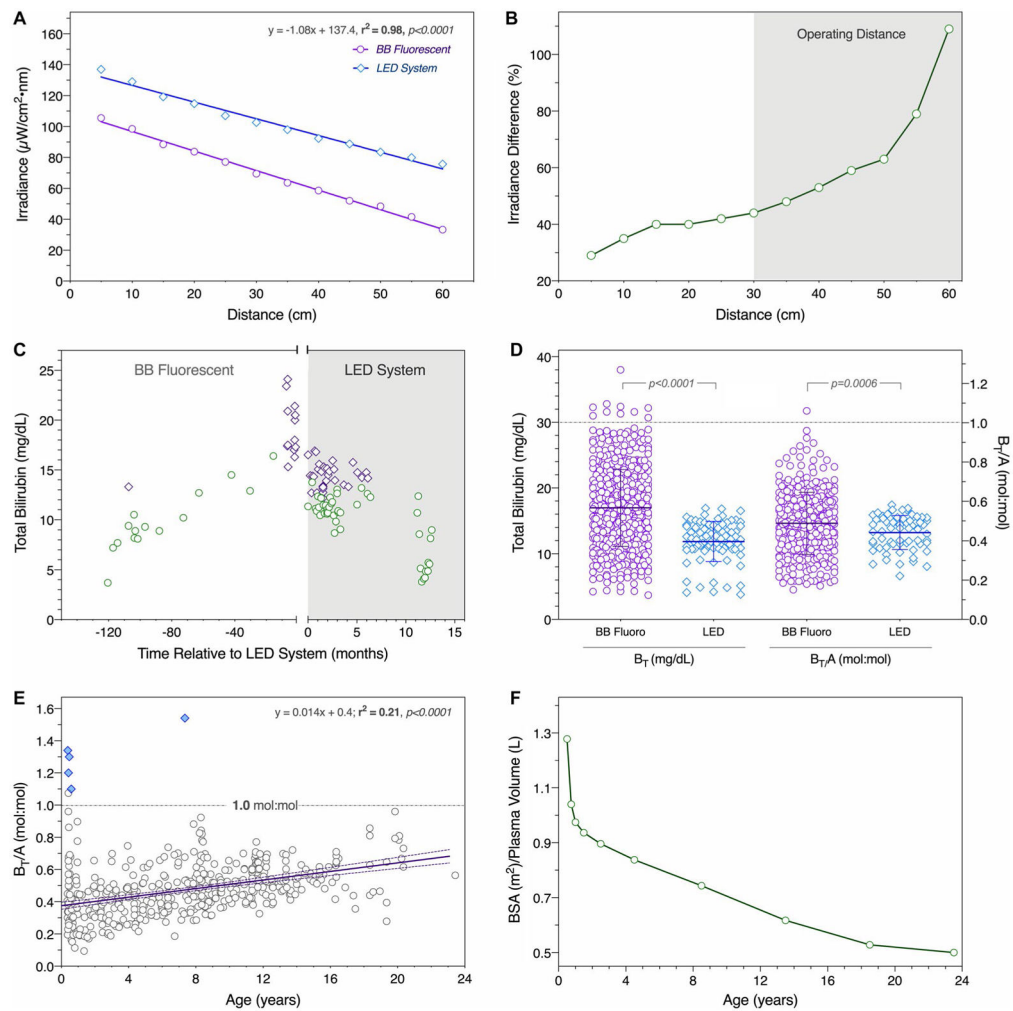


**FIG. 3.** Phototherapy. (A) For both BB fluorescent (purple circles) and LED (blue diamonds) systems, irradiance decayed as a function of distance from the source ( $r^2 = 0.98$ ,  $P < 0.0001$ ). (B) Decay was less marked for LEDs, which emitted 44%-109% higher irradiance within the standard operating range of 30-60 cm from the skin (gray background). (C) The clinical impact of this difference is shown for 2 representative *UGT1A1* c.222C>A homozygotes (indicated by green circles and purple diamonds), whose switch from the BB fluorescent (white background) to LED system (gray background) reduced serum bilirubin concentrations. (D) Total bilirubin ( $B_T$ , left y-axis) and its molar ratio to albumin ( $B_T/A$ , right y-axis) were lower in patients treated with the LED system. (E) Despite relative uniform phototherapy conditions over time, total bilirubin ( $B_T$ ) and its ratio to albumin ( $B_T/A$ ) increased with age ( $n = 28$ ;  $r^2 = 0.21$ ,  $P < 0.0001$ ; purple line with 95% confidence interval). Patients who developed kernicterus (blue diamonds) all had serum  $B_T$  concentrations that exceeded intravascular binding capacity ( $B_T/A = 1.0$  mol/mol; gray horizontal line). (F) Factors underlying this increase are an age-related decrease of “treatable” body surface area relative to plasma volume (an index of the proportional

bilirubin load exposed to blue light), increased skin thickness from infancy to adulthood, and progressive hepatopathy. Abbreviation: BSA, body surface area.

Author Manuscript

Author Manuscript

Author Manuscript

Author Manuscript

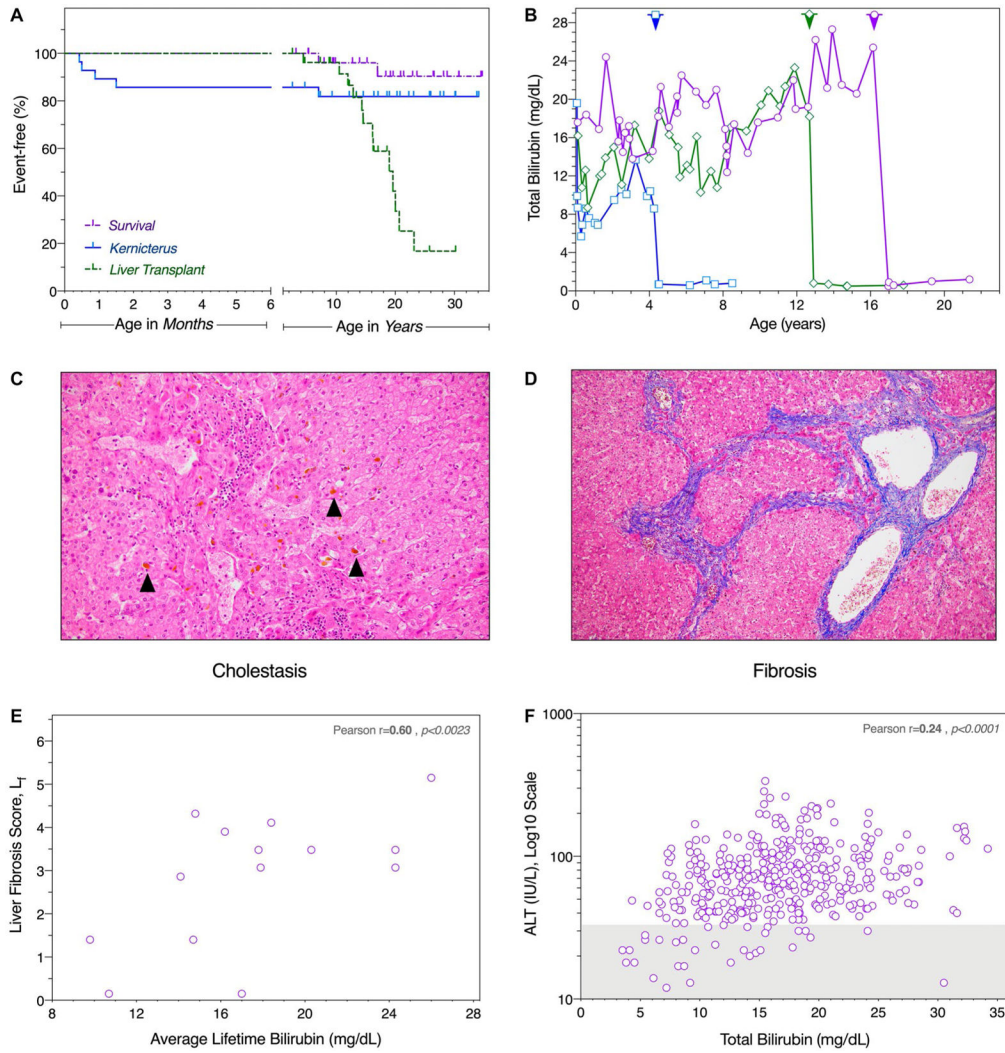


**FIG. 4.** Clinical outcomes. (A) Four of five cases of kernicterus (blue solid line) occurred within the first 6 weeks of age. Two (7%) patients died (purple dashed line): 1 from respiratory complications of neurological injury and the other from a cause unrelated to CN1 or its treatment. The youngest patient to receive a liver transplant (green dashed line) was 4.7 years old, and median age at transplant was 16.2 years. Perpendicular hatches indicate age at census. Note different scales (months and years) of the divided abscissa. (B) In all 17 transplanted patients, serum bilirubin concentration decreased within a few postoperative days and remained normal thereafter (shown for three representative cases, with timing of liver transplantation indicated by corresponding arrowhead along the upper frame). (C) Most explants showed canaliculi bile plugs (black arrows), a sign of intrahepatic cholestasis. (D) Nine (60%) livers had evidence of fibrosis ranging from mild to severe, seen here as central–central bridging on Masson trichrome stain. (E) The weighted liver fibrosis score ( $L_f$ ) correlated with serum bilirubin averaged over the patient’s lifetime ( $r = 0.60$ ,  $P < 0.0023$ ), calculated from a mean of 32 serum bilirubin levels per patient. (F) Based on data from all 28 *UGT1A1* c.222C>A homozygotes (416 paired values), there was a modest but

statistically significant correlation ( $r = 0.24$ ;  $P < 0.0001$ ) between simultaneously measured unconjugated bilirubin and alanine transaminase (ALT; log<sub>10</sub> scale). Gray shading represents the normal reference range for ALT.

TABLE 1.

## Crigler-Najjar Syndrome Management Guidelines

Principles of Effective Phototherapy	
•	<i>Light source:</i> High-intensity LED, BB fluorescent tubes, or energetic equivalent (e.g., TL52); maximum emission of 400-525 (peak 450-460) nm
•	<i>Source distance from skin:</i> 30-45 cm for infants, 45-60 cm for children and adults
•	<i>Skin exposure:</i> Body surface area exposure 60%-70% for neonates, 35%-50% for children and adults
•	<i>Exposure duration:</i> 15-20 hours per day for neonates, 7-13 hours per day for children and adults
•	<i>Surroundings:</i> White bedsheets; reflective surfaces
Treatment Goals	
•	<i>Irradiance at skin surface:</i> 40-100 $\mu\text{W}/\text{cm}^2$ per nm*
•	<i>Unconjugated bilirubin (serum/plasma):</i> 20 mg/dL (340 $\mu\text{mol/L}$ )
•	<i>Unconjugated bilirubin-albumin (<math>B_T/A</math>) molar ratio:</i> 0.7 mol:mol
–	$B_T$ in mg/dL $\times 17.1 = B_T$ in $\mu\text{mol/L}$ ; A in g/dL $\times 152 = A$ in $\mu\text{mol/L}$
–	1 g of albumin binds approximately 9 mg $B_T$
•	<i>Avoid:</i> Drugs and drug vehicles that displace bilirubin from the albumin binding site (Supporting Table S2)
Inpatient Management for Severe Hyperbilirubinemia	
•	<i>Reverse and/or prevent concomitant neurological threats, such as:</i>
–	Hypovolemia, hypotension
–	Hypercarbia, acidosis
–	Hypoglycemia, hyperglycemia
–	Hypematremia, hyperosmolarity
–	Hyperthermia
•	<i>Rule out concomitant conditions that exacerbate hyperbilirubinemia, such as:</i>
–	Hemolytic disease <sup>†</sup>
–	Internally sequestered or ingested blood <sup>‡</sup>
–	Cholelithiasis or biliary obstruction <sup>§</sup>
–	Constipation
•	<i>Provide continuous high-intensity phototherapy:</i>
–	Position the light source at minimal tolerated distance from skin



- Maximize the proportion of skin surface exposed
- Provide light exposure for about 24 hours per day.
- *Restore and maintain intravascular hydration:*
  - Intravenous normal saline (10-20 mL/kg bolus infusions) to establish euolemia
  - Intravenous dextrose in normal saline at 1 to 1.5 times maintenance rate<sup>§</sup>
  - Maintain brisk urine output
- *Prevent bilirubin displacement from albumin:*
  - Avoid pharmaceutical agents that interfere with bilirubin–albumin binding (Supporting Table S2)
  - Avoid drug combinations when possible
  - Use special caution with intravenous bolus dosing of drugs or contrast agents
- *Optimize enterohepatic lumirubin excretion:*
  - Enteral feeding: Milk-based formula in infants, lipid-rich foods in children and adults
  - Enteral calcium carbonate (MW 100): Children 2.5 mmol/kg/day, adults 100 mmol/day (TUMS [750 mg] = 7.5 mmol calcium per tablet; Roxane = 6.5 mmol per tablet)
  - For cholelithiasis and/or biliary sludging: Ursodiol (15-30 mg/kg per day); consider emergency cholecystectomy
- *Prepare for emergency measures:*
  - For B<sub>T</sub>/A 0.7: Intravenous albumin 1-2 mg/kg per dose up to 6 hours as needed
  - For B<sub>T</sub>/A 0.9: Consider exchange transfusion

---

\* Different light meters produce variable measurements from the same source. We use the BiliBlanket Meter II (GE Healthcare, Chicago, IL).

<sup>†</sup>Hemolytic conditions should be sought and treated. Consider (1) immunologic/autoimmune, (2) red blood cell enzymopathies, (3) ineffective erythropoiesis, and (4) physical destruction.

<sup>‡</sup>Internal hemorrhage, occult tissue hematoma, peripartum blood ingestion by neonates.

<sup>§</sup>10% dextrose solution for infants and toddlers, 5% dextrose for older children and adults.

Bilirubin-Albumin Binding in Serum of Control Individuals, Premature Neonates, Jaundiced Term Newborns, and *UGT1A1* c.222C>A Homozygotes

TABLE 2.

	Total Bilirubin		Albumin		Unbound Bilirubin		B <sub>T</sub> /A		K
	mg/dL	( $\mu$ mol/L)	g/dL	( $\mu$ mol/L)	$\mu$ g/dL	(nmol/L)	mol:mol	L/mol	
Amish control (n = 7)	3.8 $\pm$ 3.4	(65 $\pm$ 59)	4.8 $\pm$ 0.7	(724 $\pm$ 105)	0.06 $\pm$ 0.12	(1.0 $\pm$ 2.0)	0.10 $\pm$ 0.10	244 $\pm$ 113	
<i>UGT1A1</i> c.222C>A (n = 18)	14.7 $\pm$ 5.7	(251 $\pm$ 98)	4.4 $\pm$ 0.5	(663 $\pm$ 67)	0.42 $\pm$ 0.33	(7.1 $\pm$ 5.7)	0.38 $\pm$ 0.15	118 $\pm$ 57	
Term idiopathic jaundice (n = 8) *	30.5 $\pm$ 2.2	(521 $\pm$ 38)	3.9 $\pm$ 0.6	(583 $\pm$ 96)	3.2 $\pm$ 2.0	(54.5 $\pm$ 33.8)	0.93 $\pm$ 0.24	101 $\pm$ 36	
Preterm < 1 kg (n = 6) †	6.5 $\pm$ 2.9	(111 $\pm$ 49)	3.0 $\pm$ 0.8	(448 $\pm$ 123)	1.13 $\pm$ 0.92	(19.4 $\pm$ 15.7)	0.27 $\pm$ 0.16	28 $\pm$ 17	
ANOVA P value ‡	< 0.0001		< 0.0001		< 0.0001		< 0.0001	< 0.0001	
Amish control vs. <i>UGT1A1</i> c.222C>A	****		ns		ns		**	**	
Amish control vs. term idiopathic jaundice	****		*		****		****	**	
Amish control vs. preterm < 1 kg	ns		****		ns		ns	****	
<i>UGT1A1</i> c.222C>A vs. term idiopathic jaundice	****		ns		****		****	ns	
<i>UGT1A1</i> c.222C>A vs. preterm < 1 kg	**		****		ns		ns	*	
Term idiopathic jaundice vs. preterm < 1 kg	****		*		**		****	ns	

\* Data from Ref. 19.

† Data from Ref. 13.

‡ Tukey's *post hoc* test for multiple comparisons: ns, not significant ( $P > 0.5$ )

\*  $P$  0.5

\*\*  $P$  0.1

\*\*\*  $P$  0.001

\*\*\*\*  $P$  0.0001.

Abbreviations: BT, total bilirubin; and K, bilirubin-albumin equilibrium association binding constant.

Biochemical Measurements from *UGT1A1* c.222CA Homozygotes Under Phototherapy or Post-Liver Transplantation

TABLE 3.

Serum Measurement	Reference Range	Phototherapy (N = 28)*				After Liver Transplantation (N = 17)				P	F (P)‡		
		N†	Mean ± 1 SD	Median	Range	CV	N	Mean ± 1 SD	Median			Range	CV
Total bilirubin, mg/dL ( $\mu\text{mol/L}$ )	<0.8 (<14)	627	17.0 ± 5.9 (278 ± 100)	16.0 (274)	3.7-39.0 (63-667)	36%	113	0.9 ± 1.0 (15 ± 17)	0.7 (12)	0.2-9.8 (3-168)	108%	<0.0001	34.8 (<0.0001)
Albumin, g/dL ( $\mu\text{mol/L}$ )	3.7-5.6 (559-846)	475	4.2 ± 0.5 (627 ± 77)	4.2 (634)	2.8-6.7 (420-1,012)	12%	90	4.2 ± 0.4 (638 ± 57)	4.3 (649)	3.3-5.5 (498-831)	9%	ns	1.6 (0.0106)
Bilirubin-albumin ratio, mol:mol	—	475	0.47 ± 0.17	0.47	0.10-1.51	35%	76	0.02 ± 0.03	0.02	0.01-0.26	130%	<0.0001	28.4 (<0.0001)
Alanine aminotransferase, U/L	10-45	401	75 ± 46	66	8-333	61%	134	52 ± 126	29	10-1,427	242%	0.0405	7.5 (<0.0001)
Alkaline phosphatase, U/L	120-488	384	217 ± 60	218	38-420	28%	94	93 ± 62	76	29-469	67%	<0.0001	1.1 (ns)
Gamma-glutamyltransferase, U/L	2-39	302	33 ± 36	23	3-393	111%	125	51 ± 61	25	7-289	120%	0.0024	2.9 (<0.0001)

\*The “phototherapy” group is made up of all 28 *UGT1A1* c.222C>A homozygotes; the “post-liver transplantation” group is made up of 17 of those same individuals after they received a liver transplant.

†“N” represents the number of individual laboratory values analyzed from patients treated with phototherapy (n = 28) as compared with liver transplantation (n = 17).

‡F is the ratio of SDs squared. P represents the P value for the F ratio; it measures the probability that the SDs (i.e., variance between populations) are the same.

Abbreviations: CV, coefficient of variation; na, not applicable; ns, not significant (ANOVA  $P > 0.05$ ).

**TABLE 4.** Crigler-Najjar Syndrome Outcomes: Temporal and Geographical Patterns Over 7 Decades

Cohort	Ref.#	Nationality	Year	N	Brain Injury	Outcomes (% Affected)		
						Liver Transplant	ET or PP	Death
Crigler and Najjar <sup>*</sup>	1	United States	1952	7	100%	0%	0%	100%
van der Veere et al. <sup>†</sup>	42	International	1996	57	26%	37%	nr	9%
Suresh and Lucey <sup>‡</sup>	43, 44	International	1997	42	23%	36%	28%	0%
Shevell et al. <sup>§</sup>	45	International	1998	63	59%	8%	10%	nr
Nazer et al. <sup>  </sup>	46	Saudi Arabia	1998	12	50%	17%	50%	8%
Aloulou et al. <sup>¶</sup>	47	Tunisia	2010	30	93%	0%	0%	nr
Present study <sup>#</sup>	na	United States	2019	28	18%	61%	7%	7%
Total N/average value <sup>***</sup>				239	45%	27%	19%	8%
Range				7-63	18%-100%	0%-63%	0%-50%	0%-100%

<sup>\*</sup> Crigler and Najjar’s original report preceded the advent of exchange transfusion, plasmapheresis, phototherapy, and liver transplantation for treatment of Crigler-Najjar syndrome.

<sup>†</sup> Brain injury patients (n = 8) were transplanted later (14.3 ± 5.9 years) than those without brain damage (n = 13, 5.9 ± 5.4 years).

<sup>‡</sup> Information is compiled from an international questionnaire involving patients from four continents. There is patient overlap with other studies, including our Amish cohort (12 of the 42 patients reported). In the non-Amish subgroup, neurological disability was present in 9 of 30 patients (30%). The mean ± SD bilirubin values (in mg/dL) varied by subgroup: neonatal peak 26.6 ± 5.8, neonatal typical 19.8 ± 4.5, postnatal typical 20.5 ± 5.

<sup>§</sup> The 59% incidence of neurological injury is based on an extensive review of 37 published articles (1952-1997) by these authors, who further subdivided adverse outcomes into four discrete patterns of disability.

<sup>||</sup> Information from 5 affected siblings, not included in the 12-patient cohort, is included in the paper by Nazer et al. All 5 died with bilirubin-induced brain injury, resulting in a total brain injury rate of 10 of 17 (59%) and a disease-related mortality of 38%. Four patients required more than one exchange transfusion, for a total of 13 exchange procedures among 6 of the 12 patients reported.

<sup>¶</sup> Exchange transfusion and liver transplantation were not treatment options, and local resources did not support the use of high-intensity phototherapy at home.

<sup>#</sup> Prior to coming under our care, 2 patients in the cohort required exchange transfusion as neonates and 1 developed kernicterus. However, these outcomes were not observed for patients under our care from 1989 to present.

<sup>\*\*\*</sup> Average values are calculated from a denominator of 232 (rather than 239), accounting for the limited therapeutic options available in 1952.

Abbreviations: ET, exchange transfusion; na, not applicable; nr, not reported; PP, plasmapheresis.